Author(s): Kaukonen, M. & Peräjoki, J. & Nieminen, Risto M. & Jungnickel, G. & Frauenheim, Th.

Title: Locally activated Monte Carlo method for long-time-scale simulations

Year: 2000

Version: Final published version

Please cite the original version:

Kaukonen, M. & Peräjoki, J. & Nieminen, Risto M. & Jungnickel, G. & Frauenheim, Th. 2000. Locally activated Monte Carlo method for long-time-scale simulations. Physical Review B. Volume 61, Issue 2. 980-987. ISSN 1550-235X (electronic). DOI: 10.1103/physrevb.61.980.

Locally activated Monte Carlo method for long-time-scale simulations

M. Kaukonen, J. Peräjoki, and R. M. Nieminen
Laboratory of Physics, Helsinki University of Technology, P.O. Box 1100, FIN-02015, Helsinki, Finland

G. Jungnickel and Th. Frauenheim
Laboratory of Physics, University of Paderborn, Warburger Strasse 100, 33098 Paderborn, Germany
(Received 11 August 1998; revised manuscript received 2 July 1999)

We present a technique for the structural optimization of atom models to study long time relaxation processes involving different time scales. The method takes advantage of the benefits of both the kinetic Monte Carlo (KMC) and the molecular dynamics simulation techniques. In contrast to ordinary KMC, our method allows for an estimation of a true lower limit for the time scale of a relaxation process. The scheme is fairly general in that neither the typical pathways nor the typical metastable states need to be known prior to the simulation. It is independent of the lattice type and the potential which describes the atomic interactions. It is adopted to study systems with structural and/or chemical inhomogeneity which makes it particularly useful for studying growth and diffusion processes in a variety of physical systems, including crystalline bulk, amorphous systems, surfaces with adsorbates, fluids, and interfaces. As a simple illustration we apply the locally activated Monte Carlo to study hydrogen diffusion in diamond.

I. INTRODUCTION

The molecular-dynamics (MD) (Ref. 1) simulation method is an extremely powerful tool to study microscopic motion based on the Newtonian dynamics of atoms interacting through a model potential. The equations of motion are solved using a mesh of discrete time steps. The time step must be short compared the phonon frequencies, usually a fraction of a femtosecond. Hence, the total simulation time, which is of the order of 1000 to 100 000 steps dependent on the model potential, is only in the picosecond region. At maximum, MD methods can be used to simulate atomic processes occurring on a time scale of nanoseconds. For a variety of physical situations, however, this is far too short to study the true dynamics of a system, in particular for diffusive processes such as atom migration on surfaces, certain formation processes during growth, and defect migration in bulk material.

A recent extension of standard MD schemes due to Voter[2] focuses on the simulation of such processes. By adding an artificial boosting potential to the true local energy landscape of the atoms, the energy barriers to configurations which are normally not accessible by ordinary MD can be overcome. Thus, the atoms are forced to do movements which are related to barrier heights incompatible with normal thermal activation energies, yielding an extended time scale.

Another class of methods that has been proposed to relax a system over a large period of time is based on the knowledge of the local energy barriers. In a method by Barkema and Mousseau[3,4] the local energy barriers are explicitly searched for with an inverse conjugate gradient method using a modified force vector. Atoms are allowed to make jumps over the actual saddle points found according to a standard Metropolis Monte Carlo (MC) algorithm with a fictitious temperature (2500 K). This temperature is the parameter which controls the acceptance rate of certain relaxation processes and hence the time scale under consideration. This parameter is, however, not known *a priori* and difficult to determine. Furthermore, the method suffers from the fairly general problem whether all saddle points relevant for the evolution of the system can be found. This scheme which is known as the activation-relaxation technique (ART) has been used in identifying relevant local relaxation processes in amorphous silicon at low temperatures.[6]

If the dynamics of a system can be described as a sequence of rather independent infrequent events, long time scales can be modeled using transition-state theory (TST). Since its development in the thirties, TST has been applied to a wide range of phenomena.[7–9] Voter developed a TST based kinetic Monte-Carlo (KMC) method for describing the dynamics of such infrequent events in a regular lattice and applied it to the study of rhodium clusters on Rh(100).[10] Here, we develop a method based on similar ideas which, however, is more general and can be used to investigate diffusion reactions without assuming a regular lattice. Since this requires some knowledge of the local energy landscape in the vicinity of a moving atom it also contains features common to the ART described above.

In TST based methods, rate constants for infrequent events usually depend on the predetermination of reactants and products, e.g., on the knowledge of the local energy minima prior to and after a chemical reaction. Then, various schemes[11,12] may be applied to reach transition states which are characterized by the saddle points of the energy landscape. From this information one can extract the transition probability for an event and the related time scale. However, if significant reactions are missed initially or if the potential changes remarkably during the evolution of the system, the information gained from such simulations is quite restricted.

Our method, therefore, starts from ideas similar to ART in that we focus on the determination of the most relevant if not all energy barriers that an atom sees in its immediate neighborhood at any time the atom is going to make a move. In the locally activated Monte-Carlo (LAMC) technique,[13]

we imagine a model structure as a system for which the short range and the short medium range order[14] are the prime factors responsible for the actual form of the local potential. Therefore, we concentrate on finding the energy barriers in the vicinity of an atom and the related smallest energy paths. This is done by efficiently mapping the energy landscape in a few directions around each atom and defining a local distribution function for the probability of the atoms to escape from their current positions.

Within LAMC an event is the instantaneous jump of selected atoms called the movers over one of their nearby barriers. For this, the local distribution of escape rates determines the probability in which direction the selected atom will move. Once the escape direction is chosen due to this distribution function the transition probability is assumed to be unity. Hence, movers are forced to jump even if the energy barrier in the selected direction is rather high. Since the typical escape rate for the event is mapped there is a well-defined control over the real time scale in which this event takes place. Using the LAMC scheme together with a MD simulation introduces small random disturbances but allows to advance the clock after a jump according to the average escape rate of the mover and, therefore, extends the time scale enormously.

The paper is organized as follows. In Sec. II we present the ideas behind LAMC in more detail. As an example we discuss in Sec. III the diffusion of a hydrogen atom in diamond, which is an important process for understanding the chemical vapor deposition (CVD) frequently used to deposit diamond thin films.[15] Note that this application involves modeling of heteropolar interactions although the problem is simplified due to the homopolar symmetric host in which the hydrogen atom is allowed to move. A discussion of the power of LAMC follows in Sec. IV.

II. METHOD

In traditional TST based MC studies, the possible reactions that may occur in the system are assumed to be known *a priori*. The global evolution of the system is separated into single atom events (generic moves) for which the typical barriers are predetermined and assumed to remain unchanged as the system relaxes. Usually the barriers are calculated for the generic moves of an atom in an otherwise ideal host matrix by the most accurate methods available[16,17] before actually doing any structural optimization of the model. A Monte Carlo step consists of randomly selecting one of the atoms and one of the generic moves and of evolving the system according to the transition rate for this move. The rate is given as an exponential of its predetermined barrier height. The barrier controls the acceptance rate in much the same way as the total energy difference between the initial and a final state of the model in an ordinary Metropolis MC method.

In practical situations such as surface growth or relaxation of amorphous materials it is rather unlikely that the typical barriers remain constant over a longer period of time. Also, it is extremely difficult if not impossible to predict the most relevant generic events in particular in systems with many different types of atoms. Therefore, we present a method which within the limits of TST is suitable for the relaxation of any given structure provided the dynamical behavior becomes largely determined by infrequent events.

Classically, the fundamental assumption in TST is that there exists a dividing surface in phase space with two properties: (i) it separates reactants from products and (ii) any trajectory crossing this surface will not recross it. The related rate constants which describe the equilibrium flux of particles through the dividing surface can be approximated to a good extent by simple transition state theory (STST)[10]:

$$k_{\mathrm{STST}} = n_p \nu_0 \exp[-(E_{\mathrm{saddle}} - E_{\mathrm{min}})/k_b T], \tag{1}$$

where n_p is the number of possible exit directions, ν_0 is the harmonic frequency, E_{saddle} and E_{min} are the energies at the transition state and at the minimum, respectively, T is the temperature and k_b is the Boltzmann constant. The second basic TST assumption in practice is violated to a certain extent, since each crossing of the dividing surface does not necessarily correspond to a reactive event. Thus Eq. (1) gives an upper bound to the true rate constant. MD methods have been used to calculate dynamical corrections to STST rate by determining the fraction of TST surface crossings that lead to a true reactive event.[18] These studies show that the STST rates are very close to the dynamically exact rate constants.

Provided there exists a systematic way of finding all or at least all the lowest and significant saddle points of the energy landscape in the immediate neighborhood of an atom one would be able to evolve the system in accord with the STST expression for the rate constant. We wish to implement this idea into a Monte Carlo type algorithm which can be easily combined with MD in order to study a structure dynamically under the influence of long-term processes. Generally, there is no explicit restriction for the model potential which is used to evaluate the atomic interactions and, hence, the saddle points. The actual choice for this potential may be critical though and the most accurate quantum-chemical potentials should be given the preference. This is particularly essential in sensitive bonding situations such as in carbon when classical potentials[19–23] usually applied for large models may frequently fail to reproduce the true barriers in the structure.

For example, Tersoff's classical potential which has been applied very successfully in a number of carbon studies[21,24–26] was shown to result in additional local minima and associated barriers in the energy landscape when studying the relaxation of an hypothetical icosahedral carbon cluster.[27] In contrast, true density-functional or Hartree-Fock based self-consistent potentials require computer resources that would restrict the size of the models under consideration enormously and are almost impractical for real diffusion or growth modeling.

For the total-energy calculations in this study we therefore utilize as a reasonable compromise the recently developed density-functional based tight-binding approach (DFTB).[28,29] This method derives its name from the use of self-consistent density-functional calculations for pseudoatoms in order to construct transferable tight-binding (TB) potentials for the non-self-consistent solution of the Kohn-Sham equations of the many body system. The main idea of the scheme is to superpose local atomiclike orbitals to make up the molecular

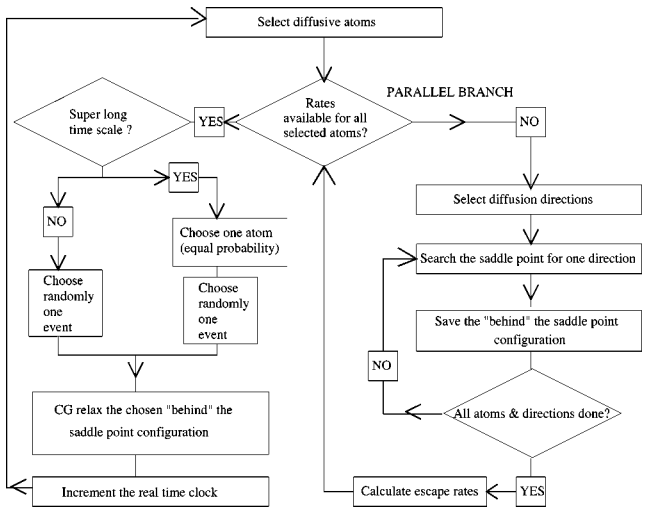

FIG. 1. The flowchart of the LAMC procedure described in Chap. II.

states where the set of local orbitals is chosen in such a way as to predict the total charge density of the full structure as well as possible. Then, the Kohn-Sham equations for the complete model need not be solved self-consistently but still give a reasonable total energy.

The DF-TB method has been successfully applied to various carbon systems, ranging from small clusters[28,30] to buckminster fullerenes and related oligomers,[31] amorphous carbon systems,[32] and carbon surfaces.[33–35] Moreover, heteropolar interactions of carbon with hydrogen, boron, and nitrogen have been modelled accurately with this technique.[35–37] A flow chart of the LAMC method that we introduce is presented in Fig. 1 and will be discussed below.

A. Choice of the diffusing atoms

In general all atoms in a given model structure may be involved in infrequent jumps (diffusive events) over barriers in their neighborhood. The number of atoms that are explicitly considered may be restricted in order to study only such processes that are associated with a certain atom type or a subregion of the full model (such as a surface). In the following those atoms where events are initiated are called the movers which does not mean that the remaining atoms in the system are kept fixed at their positions. The number movers will be designated by N_{diff}. The reason for these definitions is to prevent other events such as the self-diffusion in the bulk from interfering with the particularly interesting cases such as the migration on a surface.

B. Choice of the global search directions

The definition of general search directions $r^i_{\mathrm{direction}}$ for which events may take place is a central feature of our method. We will call such a direction a diffusion direction hereafter although we do not necessarily restrict the scheme to diffusion in the classical sense. Diffusion directions may be assigned to any of the N_{diff} atoms. The maximum number of the possible diffusion directions per atom n^i_{dd} basically determines whether we are able to find all the local barriers that an atom sees when being activated from its harmonic basin in the energy landscape. To avoid extensive calculations, however, we consider this number n^i_{dd} to be finite and small. The n^i_{dd} search directions are obtained in the following way: take a random diffusion direction; the rest n^i_{dd-1} directions are chosen by uniformly sampling an imaginary sphere around the moving atom.

The total number of search directions determines the success rate with which one will be able to find all or at least the essential local barriers in the next step of LAMC. The n^i_{dd} for each mover can be made to depend on the local geometry around the mover, for example, n^i_{dd} may depend on the number of the nearest neighbors of the mover.

C. Search for the saddle points

1. Finding true diffusion barriers by the projected conjugate gradient (PCG) method

The global search directions defined so far in general do not contain the true barriers of the system although the saddle points are expected to be close, in particular when the number of search directions is large. To find the relevant diffusion barriers we utilize a method recently introduced to specify changes in barrier heights on top of diamond surfaces due to the presence of dopants in subsurface layers.[35] In this particular scheme single energy barriers are found by a series of conjugate gradient (CG) relaxation processes with modified forces for the diffusing atom. The principle is similar to what has been introduced to ART.[3,4] In our method, however, the force on the diffusing atom is projected onto equidistant planes which are always perpendicular to the global search direction. Therefore, the diffusing atom can only relax within these virtual planes, whereas all other atoms can fully relax due to the true interatomic forces acting on them.

Between two consecutive CG steps the diffusing atom is pushed from the current to the next plane on a straight line connecting the position in the current plane with the final point on the global search direction. Then the whole system is CG relaxed under the restrictions described above.

Note that all atoms can react to the changes in the position of a single mover and that the particles can even get around huge barriers that may exist along the global search direction. Figure 2 shows a snapshot of a typical situation when searching for a single barrier. The solid circles indicate the initial and final position of the moving atom, dotted circles mark its positions along the migration path at various steps of the calculation. The start and end points along the global search direction which is marked by the straight dashed line for the ith single mover are indicated by $\vec{r}^{\,i}_{\mathrm{initial}}, \vec{r}^{\,i}_{\mathrm{final}}$, respectively. The relaxed position of the mover in one of the planes is $\vec{r}^{\,i}_{\mathrm{current}}$.

As discussed above, in any diffusion step the mover is initially set to the crossing point of the next plane along the global search path and the vector $\vec{r}^{\,i}_{\mathrm{final}} - \vec{r}^{\,i}_{\mathrm{current}}$. Therefore, the mover will be always focused back onto the global search direction so that the search path cannot diverge which is the major difficulty in another study[5] that attempts to find all the local barriers. The position of atom i in the next virtual plane is given by

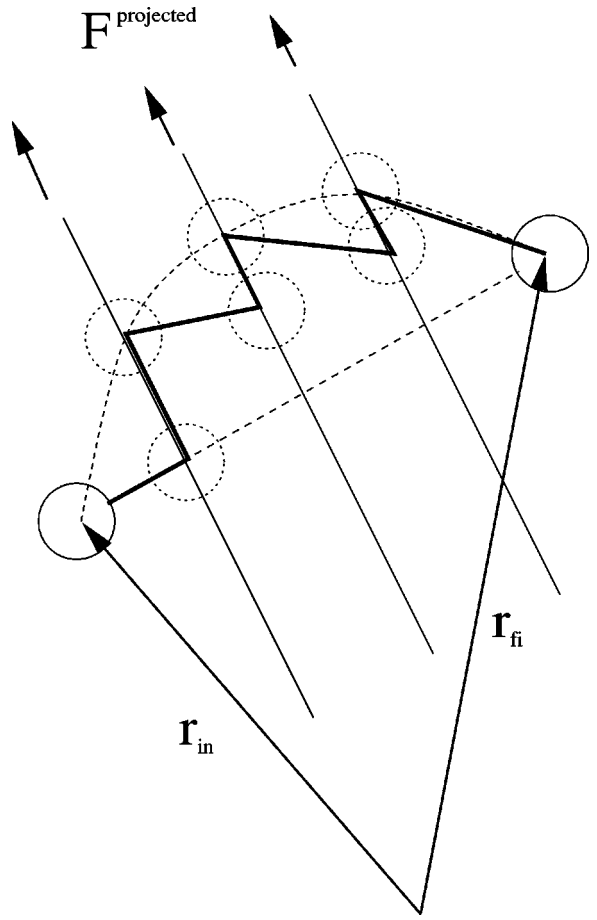

FIG. 2. The projected conjugate gradient method. Here the diffusing atom is moved in four steps from the initial position r_{in} to final position r_{in}. Forces $F_{\text{projected}}$ acting on the diffusing atom are restricted to the planes perpendicular to the diffusion direction during the CG minimization.

$$\vec{r}^{\,i}_{\text{next}} = \vec{r}^{\,i}_{\text{current}} + \frac{\vec{r}^{\,i}_{\text{final}} - \vec{r}^{\,i}_{\text{current}}}{n_{\text{total}} - n_{\text{current}}}, \tag{2}$$

where n_{total} is the total number of steps between the initial and the final point along the global search direction. This is the parameter which determines the accuracy of the barrier height finally found. It is chosen such that the step length (i.e., the distance between the adjacent planes in Fig. 2) $\vec{r}^{\,i}_{\text{final}} - \vec{r}^{\,i}_{\text{initial}}/n_{\text{total}}$ becomes so small that the desired accuracy in the height of the energy barrier can be obtained.

There is a certain degree of freedom how to pick the final position of a mover along a selected global search direction. In order to make the algorithm very much independent of this choice the position is set quite far away (>100 Å) from the initial local minimum. This is possible since the search for saddle points in the vicinity of the global search direction is terminated as soon as the first relevant saddle is found. The maximum number of search steps determines the distance between the virtual planes that restrict the motion of the mover. For the example in Sec. III we used $\vec{r}^{\,i}_{\text{final}} - \vec{r}^{\,i}_{\text{current}} = 100$ Å, $n_{\text{total}} = 2000$ yielding a spacing of 0.05 Å .

The number of search steps already made (n_{current}) ranges from zero to $n_{\text{total}} - 1$. The single search step is finished by relaxing the system with the CG method allowing all atoms in the structure to change their positions while constraining the mover onto the plane perpendicular to $\vec{r}^{\,\text{initial}} - \vec{r}^{\,\text{final}}$. The projected force for such a diffusing atom is calculated as

$$F^k_{\text{projected}} = F^k - (r^k_{\text{final}} - r^k_{\text{initial}}) \frac{(\vec{F} \cdot \vec{\Delta r})}{|\vec{\Delta r}|^2}, \tag{3}$$

where $\vec{\Delta r} = \vec{r}_{\text{final}} - \vec{r}_{\text{initial}}$, and k denotes the $x,y,$ or z coordinates. The projected force is substituted for the true total force acting on the diffusing atom. After this procedure the CG total energy minimization operates in the usual way. Note also that projecting forces before actually calling the CG algorithm is sufficient for all of the subsequent CG steps since the conjugated directions constructed during the minimization of the energy functional depend linearly on the initial data.

The method enables us to find a minimum-energy path related to any of the given global search directions independently. Therefore, the scheme can take full advantage of parallel computer architectures. If the initial position of a mover is a local minimum this path must either contain at least one saddle point to overcome or the total energy increases steadily.

2. Finding the saddle point configurations

The saddle points are searched by moving diffusing atoms or movers along global search directions as described above. The movement of a single mover is continued until (i) a saddle point is reached with an energy at least $\delta E_{\min}$ higher than the total energy at the starting point or, (ii) the total energy becomes ''much'' larger ($\delta E_{\max}$) than the initial energy. For this work, $\delta E_{\min}$ and $\delta E_{\max}$ were chosen to be 0.2 and 7.0 eV, respectively.

The saddle point position of the ith mover $\vec{r}^{\,i}_{\text{saddle}}$ is defined as the position vector of atom i where the total energy decreases for the first time after leaving its initial position. The lower limit $\delta E_{\min}$ is used to suppress very frequent events. The detailed study of the short term behavior of the system is the standard task of ordinary MD simulations. Here, this limitation was set to 0.2 eV and we investigated migration processes with exceeding barriers. Therefore, large escape rates associated with the smallest energy barriers do effectively not contribute to the time scale. For case (ii), any k_{esc} attributed to associated directions is set to zero. The N_{saddle} saddle point positions $r^{(i,j)}_{\text{saddle}}$ and $k^{(i,j)}_{\text{esc}}$ are saved.

D. Choice of a diffusion event

After determination of the

$$N_{\text{saddle}} = \sum_{i=1}^{N_{\text{diff}}} n_{dd}(i) \tag{4}$$

saddle points related to the events (i.e., all the barriers which surround all atoms declared to be movers), the escape rates k^i_{esc} are calculated using Eq. (1) assuming that the attempt frequency ν is the same for all events. In principle it is possible to estimate the true attempt frequency for each process using the harmonic approximation.[10] This calculation of ν_0, however, is demanding and beyond the current computer re-

sources. The number of diffusion directions n_{dd}^{i} which are taken into account for an atom i is only restricted by the computer power. It may depend on the local atomic geometry.

The saddle points found for each global search direction of every mover define a set of local escape rates of the atoms from their harmonic basins. This set of escape rates can be regarded as a distribution function from which the most popular event, i.e., a mover plus its escape direction can be found by drawing with a probability given by the distribution function.

In the simplest variant, the selection of the diffusing atom, the ''mover,'' and its diffusion direction, is a single step process. The particular diffusion event is selected from the pool of all possible ones by weighting the selection with the probability of the jump. In this way the physical reactions which can occur within the predefined energy window of the saddle points $\delta E_{\min} < E_{\text{saddle}} < \delta E_{\max}$ are explicitly taken into account in the STST-way according to Voter.[10] Here, lower lying saddle points are more frequently chosen than others which may be a deficiency in particular in heteropolar or inhomogeneous systems. In the worst situation the time increments are always almost the same and only a subset of events is considered. The evolution of the system may then become artificially confined to a small part of the full system.

In contrast, to increase the importance of slower events for the evolution of the system the procedure may be altered to a random selection of the mover followed by drawing the event in accord with the pool of the escape rates of the selected mover. So the sum in Eq. (5) is restricted to the diffusion directions belonging to the selected single mover only. All the diffusing atoms have the same probability to be chosen for the mover and the fluctuation of time increments after completed diffusion jumps becomes remarkable [Eq. (5)]. Here, the long term evolution is governed by the diffusion events with large barriers and rapid diffusion events are partially suppressed. However, when choosing this ''superlong'' time scale, the detailed balance condition is lost. Thus the ensemble averages cannot be accumulated in a reliable way. We note that the energy window has the role of a time filter in a way similar to previous KMC studies.[38,39]

E. Completion of the event

After the event has been chosen the chosen atom is set to the precalculated (Sec. II C) saddle point position $r_{\text{saddle}}^{(i,j)}$ (i.e. slightly behind the saddle point, as defined in Sec. II C). Thereafter the whole structure is CG relaxed without any further restriction or modifications of the forces in order to find the final state after the successful diffusion event. Placing the mover at the actual saddle point is the activation step of the event in the ART terminology.

The time dimension can be included into the simulations, if the attempt frequency ν_0 in Eq. (1) is known from either experiments or calculations of the vibrational spectra at the local minima and the saddle point configurations. The clock is incremented after an event by

$$\Delta t_{\text{hop}} = \left[\sum_{j=1}^{n_{dd}} k_{\text{esc}}^{j} \right]^{-1}, \tag{5}$$

where the index j includes the diffusion directions of the atom which made the most recent jump. k_{esc} is the same as k_{STST} in Eq. (1), except that the number of possible exit directions n_p is set to one because all the saddle points are searched individually. This time increment Δt_{hop} yields a lower limit of the time duration while it assumes that any of the diffusion jumps has taken place. An alternative way to define the time increment is given by Battaile *et al.*[17] However, in the LAMC, the pool of the escape rates may change after every diffusion jump, so it is not clear that the time increment suggested by Battaile *et al.* converges to the correct value.

F. Update of the distribution of escape rates

For those atoms whose local environment changes considerably due to the diffusion event the local escape rates need to be updated before drawing from the pool of escape rates again in order to define the next successful event. This is done in the same way as described above in Secs. II A, II B, and II C. The update is only necessary for atoms that changed their coordination numbers in the recent event remarkably or that have moved during the subsequent CG steps more than a critical distance. Note that atoms may change their status from being defined as ''movers'' to ''nonmovers'' or vice versa during the simulation according to the definition of a mover.

III. SIMULATION DEMONSTRATIONS

A. Results for hydrogen diffusion in diamond

To illustrate our LAMC method we study hydrogen diffusion in diamond. We consider this process as a sequence of uncorrelated jumps from one interstitial site to another. A single hydrogen atom is moving between 64 carbon atoms enclosed in a cubic cell with periodic boundary conditions. Thus, the number of diffusing atoms N_{diff} (Sec. II A) is just one. The number of global diffusion directions per atom n_{dd} (Sec. II B) is set to six. The first initial diffusion directions (Sec. II B) is selected randomly and the rest five are sampled uniformly on an imaginary sphere. The six virtual final points $\vec{r}_{\text{final}}$ (Sec. II C) are selected to be points towards the six initial diffusion directions and 100 Å away from the diffusing atom. The total number of diffusion n_{total} steps is set to 2000, yielding the spacing of 0.05 Å between the PCG planes (Sec. II C and Fig. 2). Six carbon atoms on the faces of the supercell are fixed to prevent a center of mass motion. This leads to higher energy barriers at the boundary of the supercell and to an artificial reflection of the diffusing atom. These effects do not change our conclusions significantly. An alternative way to prevent the motion of the supercell is to add a constant force component to all atoms in the supercell after the true forces are calculated.

The properties of interstitial hydrogen in diamond have been studied earlier by Estle *et al.*[40] at the approximate *ab initio* Hartree-Fock level with the method of partial retention of diatomic differential overlap (PRDDO), representing the bulk host by small saturated cluster models. Their calculations indicate that the lowest-energy site for hydrogen is an interstitial in the relaxed bond-centered (BC) site which appears to be 2.7 eV below the tetrahedral (T) site. By linear

TABLE I. Energies of various sites for H relative to the energy at a BC site and the energy barriers. All energies are in eV.

	This Work	Ref. 40	Ref. 42	Ref. 41	Ref. 43
ΔE_T	1.6±0.1	2.7	5.3[a]	2.7	1.9
ΔE_{AB}	1.7±0.1				
$E^{\mathrm{barr}}_{T\text{-to-BC}}$	0.4±0.1	5.1		2.5	
$E^{\mathrm{barr}}_{\mathrm{BC\text{-}to\text{-}BC}}$	2.6±0.1		1.9		
$E^{\mathrm{barr}}_{T\text{-to-AB}}$	0.4±0.1				
$E^{\mathrm{barr}}_{\mathrm{AB\text{-}to\text{-}BC}}$	0.2±0.1				

[a]T site is not stable.

interpolation between the atomic positions of the relaxed BC and T site models, they could estimate the barrier inbetween to be of the order of 5 eV.

The BC site has also been found more stable compared to the T site by Chu *et al.*[41] on the same level of theory using saturated cluster models containing up to 44 carbon atoms. There, however, the barrier between the BC and the T site has been determined to be only about 2.5 eV above the BC site.

A barrier of about 1.9 eV has been determined for the migration from one BC site to a neighboring BC site in the study by Mehandru *et al.*[42] using the semiempirical atom superposition and electron-delocalization molecular orbital technique with a 46 C-atom cluster model. The density-functional pseudopotential self-consistent field calculation using the local-density approximation (SCF-LDA) calculation by Briddon *et al.*[43] utilizing a $C_{26}H_3O$ cluster model focuses on the stability of molecular hydrogen inside the diamond crystal. For monatomic hydrogen they find the BC site to be more stable compared to the T site by 1.9 eV. The site energies and related barrier heights are summarized in Table I and compared to values obtained in the previous studies.

We started our investigation with the determination of the equilibrium configurations for hydrogen in either the interstitial BC or the T site by CG relaxing idealized geometries, allowing all the atoms in the system to relax. When hydrogen is in the BC site relaxation forces the C-C bond containing the hydrogen atom in the middle to stretch by 0.80 Å giving rise to C-H distances of 1.17 Å . The C-C distance is 52% greater than the normal bond which is slightly larger than previously reported by Estle *et al.*[40] (42%), Mehandru *et al.*[42] (43.5%), and Briddon *et al.*[43] (43%). Within DF-TB the BC site is more stable than the T site by 1.6 eV. This energy difference is about 1 eV lower than found in the Hartree-Fock calculations[40] but in very good agreement with the SCF-LDA results.[43]

We then applied the PCG algorithm to the calculation of the characteristic barriers separately. Our calculations do not fully support the results by Mehandru *et al.*[42] with respect to the transition from a BC to a neighboring BC site. The barrier appears to be about 30% higher than previously reported and seems to be the most unlikely transition compared to the other pathways between T and antibonding (AB), AB and BC, or T and BC sites. The latter three barriers are almost isoenergetic and about 2 eV lower than the former saddle point. This strongly suggests that the diffusion of hydrogen in diamond does not occur between neighboring BC sites. The BC sites self-trap hydrogen and can additionally bind other H's in a nearby AB configuration.[43] This causes hydrogen to stay at BC sites for longer periods than at T or AB sites. After activation into one of those configurations H has almost equal chances to rapidly diffuse between them or back to a BC site where it is trapped again. This appears to be consistent with the picture for silicon.[41,44]

On the diffusion path from the BC site to the T site the hydrogen atom maintains its bonding to one of the two neighboring C atoms with an increasing bond length (from 1.1 to 1.3 Å). The energy barrier is reached close to (within 0.25 Å) the T site. This saddle point configuration is characterized as a stretched tetrahedron with a H atom in the middle. The nearest neighbor H-C distances are about 1.3, 1.5, 1.7, and 1.8 Å .

Note that within our method the system is continuously relaxed during the search of the saddle points and that it may be viewed as a search with least constraints. Typically, the relaxations are of the order of 0.4 Å for the C atoms neighboring the BC hydrogen and 0.1 Å for C atoms closest to the hydrogen at a T site. Therefore, it is not surprising that the barriers are noticeably lower than in the previous studies by Estle *et al.* and Chu *et al.*, where a linear interpolation technique to constrain the geometries was applied to find upper limits for the transition state energies.

When studying the evolution of the system with the LAMC algorithm, diffusion takes place mostly between BC and T sites as expected. During a simulation of 20 diffusion jumps, only once a different state was reached. This new configuration is of particular interest and will be called the antibonding site which has not been observed for monatomic hydrogen in diamond before. For silicon the same configuration has been determined to be a local minimum[44] in the energy landscape, too.

The AB state occurs when the hydrogen atom is neither in an exact bond-centered nor a tetrahedral position. The AB state is reached by moving the H atom 0.15 Å from the tetrahedral position to the (111) direction. The neighboring C atom in this direction moves towards the H atom yielding a true C-H bond of 1.08 Å. The AB site is only marginally (0.1 eV) higher in energy than the T site, and the barrier from a T site to the AB site is found to be 0.4±0.1 eV.

We calculated the vibrational spectra for the BC and T sites, as well as for the transition-state between them, in order to get the attempt frequencies for BC to T and T to BC reactions. Equation (1) yields $k_{\mathrm{BC\text{-}to\text{-}}T}=4\times7.76\times10^{12}\times\exp(-2.0\ \mathrm{eV/kT})(1/s)$ and $k_{T\text{-to-BC}}=6\times1.16\times10^{13}\times\exp(-0.4\ \mathrm{eV/kT})(1/s)$. At 1100 K these result to $k_{\mathrm{BC\text{-}to\text{-}}T}=21360(1/s)$ and $k_{T\text{-to-BC}}=7.02\times10^{11}(1/s)$. With this information the diffusion constant can be estimated as[44,45]

$$D=\frac{1}{6}\sum_{i,j}|R_i-R_j|^2 n_i k_{ij}, \tag{6}$$

where n_i is the probability for the hydrogen atom to be located at a given site in the lattice.

Here $n_{\mathrm{BC}}=\frac{16}{24}$, $n_T=\frac{8}{24}\times\exp(-1.6\ \mathrm{eV/kT})=1.56\times10^{-8}$ at 1100 K, and $R_i-R_j=R_T-R_{\mathrm{BC}}=1.47$ Å. We thus arrive at an estimate of $D\approx9.0\times10^{-13}\ \mathrm{cm}^2/s$.

The diffusion constant D can be evaluated another way by calculating it directly from

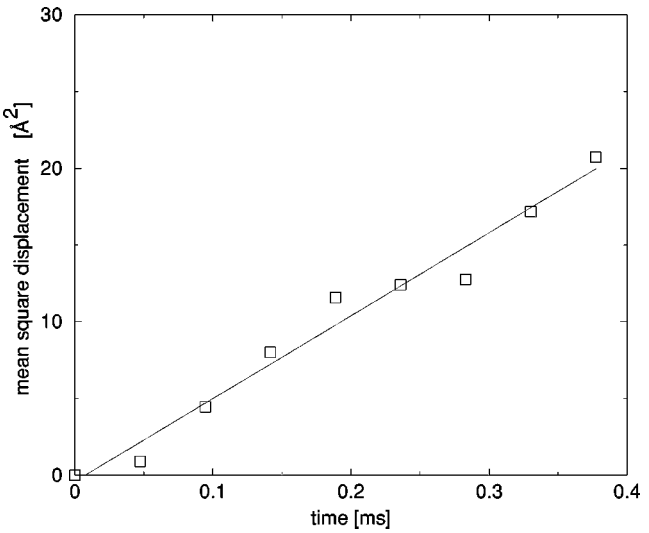

FIG. 3. The square of the displacement of the hydrogen atom in diamond; only BC sites are included.

$$D=\frac{1}{6}\lim_{t\to\infty}\left\{\frac{d}{dt}\langle[x(t)-x(0)]^2\rangle\right\}, \tag{7}$$

where the average is an ensemble average. The time evolution of the square of the displacements of the diffusing H atom is shown in Fig. 3. In this evaluation only the BC positions are taken into account. By calculating the diffusion constant from Eq. (7) we obtain again $D\approx 9.0\times 10^{-13}\mathrm{cm}^2/\mathrm{s}$. This is expected since the Eqs. (6) and (7) should give the same result when the simulation time approaches infinity. The Eq. (7) is of course more convenient in a general diffusion case when neither the diffusion paths nor the metastable states are known *a priori*.

Our estimated diffusion constant for the ideal crystalline host is about three times larger than experimental values.[46] However, in experiments diamond contains point defects, such as vacancies, impurities, and grain boundaries. The BC interstitial itself has a partially filled level close to the conduction band which becomes filled when a second hydrogen in an AB type of configuration or other impurities such as nitrogen are present nearby.[43] Hence, lattice defects can trap a diffusing H atom and thus reduce its diffusion rate.

B. Self-interstitial diffusion in silicon

Additionally we have simulated the self-interstitial diffusion in silicon. The supercell consists of 65 atoms. Two energy minima are found during a six diffusion jump LAMC run. The lower in energy corresponds the $\langle 110\rangle$ split interstitial with Si atom separation 2.26 Å, in good agreement with tight-binding calculations by Munro *et al.*[47] Our second minimum resembles the $\langle 1033\rangle$ split interstitial by Munro *et al.*, the Si atom separation being now 2.22 eV. The pathway between these two minima involves a bond rotation, which was also found to be the lowest energy pathway by Munro *et al.* (they use eigenvector following approach to find the saddle points). We find that the $\langle 110\rangle$ split interstitial lies 0.41 eV deeper in energy (Munro *et al.* 0.56) compared to the $\langle 1033\rangle$ split interstitial. Moreover, our barrier from $\langle 110\rangle$ split to $\langle 1033\rangle$ split is 0.53 eV (Munro *et al.* 0.60) and to the reverse direction 0.12 eV (Munro *et al.* 0.03 eV). However, the supercell in the calculations by Munro *et al.* consists of 216 atoms compared to ours of 64. These results demonstrate that the current method can also handle diffusion processes involving bond rotation.

IV. DISCUSSION

Finally, we wish to summarize the benefits of the LAMC method. The scheme does not require assumption about the underlying lattice structure or a list of possible chemical reactions. It is easy to parallelize since atomic jumps are assumed to occur in an uncorrelated manner and, hence, the determination of atomic escape rates can be done separately for each mover and every global search direction.

Within this technique the time scale of a simulation is spread so that a much longer process time can be achieved compared to ordinary MD. The increase of time scales depends only on the height of the true energy barriers of the system under consideration and there is no uncertain parameters such as boosting potentials or artificial activation energies needed to evolve a system.

We illustrated the method by a simple investigation of hydrogen diffusion in a diamond lattice. The relevant stable (BC) and metastable (T,AB) states have been found. Additionally, we determined the antibonding monatomic state to be metastable which has not to our knowledge been discussed prior to this work to be present in diamond and competitive with the T site. We determined the diffusion paths (BC-to-T, T-to-BC, and an antibonding pathway) and calculated the diffusion constant for H diffusion in diamond in two ways [Eqs. (6) and (7)].

The major limitation of the method is the underlying transition state theory assumption that atomic jumps occur infrequently and uncorrelated, i.e., a moving atom does not directly feel the dynamics of other jumps. Hence, collective transitions are unlikely to occur. However, since LAMC after picking a transition state from the pool of saddle points utilizes a CG relaxation to reoptimize the local geometries immediately after a successful atom jump, many-atom jumps can be induced. To directly treat the many-atom jumps increases the number of diffusion events dramatically and complicates the saddle point search enormously. However, by coupling LAMC with an augmented Lagrangian penalty method[48] this is in principle possible.

A secondary but minor deficiency is the need to define a suitable energy window for the saddle points. This depends largely on the application. The lower limit for the saddle points to become relevant inside LAMC determines whether short term processes will dominate the evolution of the structure. If this limit is too high essential physical information may be lost. The upper limit rules out processes taking place in a too long time scale. We strongly suggest to combine LAMC responsible for slow transitions with the MD technique which handles the faster motion of the atoms in a deterministic way. During growth simulations, for example, collision events and short time evolution due to subsequent relaxations may be done by MD. The long time scale relaxations between two deposition events after the short MD period may be investigated by LAMC.

A standard problem of transition state theory based simu-

lations is the uncertainty about the number of relevant saddle points when calculating escape rates. Within LAMC the number of saddle points considered simply depends on the number of global search directions and the predefined energy window. Hence, it is only a question of the available computer resources to sample the realistic distribution of escape rates for a given mover.

Finally we would like to remark that the computational efforts of the LAMC method can be dramatically reduced due to a smart choice of the set of the diffusing atoms. While in studies of disordered materials every single atom needs to be handled by LAMC, this is not very useful when the application itself provides reasons to restrict the number of diffusing species such as on surfaces. If LAMC would work on all atoms in the latter case those of the bulk material due to the higher energy barriers would influence the long time scale behavior of the system and the surface reactions of interest. In contrast, mixing of time scales may be important for studying processes at interface structures or in heterogeneous systems where different atom types can cause a superposition of quite different time scales.

ACKNOWLEDGMENTS

This research has been supported by the Academy of Finland. We acknowledge the generous computer resources of the Center of the Scientific Computing, Espoo, Finland.

[1] A.P. Smith, S. Brown, and C. Green, Phys. Rev. B **26**, 1 (1982).
[2] A. Voter, J. Chem. Phys. **106**, 4665 (1997).
[3] G.T. Barkema and N. Mousseau, Phys. Rev. Lett. **77**, 4358 (1996).
[4] N. Mousseau and G.T. Barkema, Phys. Rev. E **57**, 2419 (1998).
[5] M.I. Dykman, P.V.E. McClintock, V.N. Smelyanski, N.D. Stein, and N.G. Stocks, Phys. Rev. Lett. **68**, 2718 (1992).
[6] G. T. Barkema and N. Mousseau, Phys. Rev. B (to be published).
[7] S. Glasstone, K. Laidler, and H. Eyring, *The Theory of Rate Processes* (McGraw-Hill, New York, 1941).
[8] G. Vineyard, J. Phys. Chem. Solids **3**, 121 (1957).
[9] M. Gillan, Phys. Rev. Lett. **58**, 563 (1987).
[10] A. Voter, Phys. Rev. B **34**, 6819 (1986).
[11] S. Chekmarev, Chem. Phys. Lett. **227**, 354 (1994).
[12] J. Simons, P. Jorgensen, H. Taylor, and J. Ozment, J. Phys. Chem. **87**, 2745 (1983).
[13] A Fortran 90 skeleton of the algorithm can be obtained through anonymous ftp at hugo.hut.fi (login: anonymous, password: your e-mail address, cd pub/outgoing, get lamc.tar.gz, bye).
[14] S. R. Elliott, *Physics of Amorphous Materials* (Longman Scientific and Technical, New York, 1990).
[15] K. Kobashi, K. Nishimura, Y. Kawate, and T. Horiuchi, Phys. Rev. B **38**, 4067 (1988).
[16] E. Kaxiras, Thin Solid Films **272**, 386 (1996).
[17] C.C. Battaile, D.J. Srolovitz, and J.E. Butler, J. Appl. Phys. **82**, 6293 (1997).
[18] A. Voter and J. Doll, J. Chem. Phys. **82**, 80 (1985).
[19] S. Erkoc, Phys. Status Solidi B **152**, 447 (1989).
[20] K.E. Khor and S. Das Sarma, Phys. Rev. B **38**, 3318 (1988).
[21] J. Tersoff, Phys. Rev. Lett. **61**, 2879 (1988).
[22] D.W. Brenner, Phys. Rev. B **42**, 9458 (1990).
[23] M.I. Heggie, J. Phys.: Condens. Matter **3**, 3065 (1991).
[24] J. Tersoff, Phys. Rev. B **44**, 12 039 (1991).
[25] H.-P. Kaukonen and R.M. Nieminen, Phys. Rev. Lett. **68**, 620 (1992).
[26] G. Benedek, E. Galvani, S. Sanguinetti, and S. Serra, Chem. Phys. Lett. **244**, 339 (1995).
[27] M.I. Heggie, C.D. Latham, R. Jones, and P.R. Briddon, Phys. Rev. B **50**, 5937 (1994).
[28] D. Porezag, Th. Frauenheim, Th. Köhler, G. Seifert, and R. Kaschner, Phys. Rev. B **51**, 12 947 (1995).
[29] G. Seifert, D. Porezag, and Th. Frauenheim, Int. J. Quantum Chem. **98**, 185 (1996).
[30] P. Blaudeck, Th. Frauenheim, G. Jungnickel, and U. Stephan, Solid State Commun. **85**, 997 (1993).
[31] G. Jungnickel, D. Porezag, Th. Köhler, Th. Frauenheim, and M. R. Pederson, *Fullerenes and Fullerene Nanostructures* (World Scientific, Ltd., Singapore, 1996), p. 305.
[32] Th. Frauenheim, G. Jungnickel, Th. Köhler, and U. Stephan, J. Non-Cryst. Solids **182**, 186 (1995), and references therein.
[33] G. Jungnickel, D. Porezag, Th. Frauenheim, M.I. Heggie, W.R.L. Lambrecht, B. Segall, and J.C. Angus, Phys. Status Solidi A **154**, 109 (1996).
[34] Th. Frauenheim, Th. Köhler, M. Sternberg, D. Porezag, and M.R. Pederson, Thin Solid Films **272**, 314 (1996).
[35] M. Kaukonen, P. Sitch, G. Jungnickel, R.M. Nieminen, S. Pöykkö, D. Porezag, and Th. Frauenheim, Phys. Rev. B **57**, 9965 (1998).
[36] G. Jungnickel, Th. Frauenheim, D. Porezag, P. Blaudeck, U. Stephan, and R.J. Newport, Phys. Rev. B **50**, 6709 (1994).
[37] F. Weich, J. Widany, and Th. Frauenheim, Phys. Rev. Lett. **78**, 3326 (1997).
[38] E.J. Dawnkaski, D. Srivastava, and B.J. Garrison, J. Chem. Phys. **104**, 5997 (1996).
[39] M.M. Clark, L.M. Raff, and H.L. Scott, Comput. Phys. **10**, 584 (1996).
[40] T.L. Estle, S. Estreicher, and D.S. Marynick, Phys. Rev. Lett. **58**, 1547 (1987).
[41] C. Chu and S. Estreicher, Phys. Rev. B **42**, 9486 (1990).
[42] S.P. Mehandru, A.B. Anderson, and J.C. Angus, J. Mater. Res. **7**, 689 (1992).
[43] P. Briddon, R. Jones, and G.M.S. Lister, J. Phys. C **21**, L1027 (1988).
[44] P. Deák, L.C. Snyder, and J.W. Corbett, Phys. Rev. B **37**, 6887 (1988).
[45] A. Voter, Phys. Rev. Lett. **63**, 167 (1989).
[46] G. Popovici, R. Wilson, and S. Khasawinah, J. Appl. Phys. **77**, 5103 (1995).
[47] L.J. Munro and S.J. Vales, Phys. Rev. B **59**, 3969 (1999).
[48] M. S. Bazaraa, H. D. Sherali, and C. M. Shetty, *Nonlinear Programming, Theory and Algorithms* (Wiley, New York, 1993).